[3] Kish, R., Andryk, Ye., Mirutenko, V. (2006). Biotopy Natura 2000 na Zakarpatskij nyzovyni. Uzhgorod: Mystetska linia, 63.

[4] Katsuliak, Yu. D. (2007). Vidtvorennia dubovyh lisiv u Peredkarpatti. Kharkiv, 20.

[5] Stojko, S. M., Yashchenko, P. T., Kagalo, O. O. (2004). Rarytetnyj fitogenofond zahidnyh regioniv Ukrainy. Lviv: Liga-Pres, 232.

[6] Stojko, S. M. (2008). Zberezhennia biologichnogo bioriznomanittia ta ecologichnogo balansu I pidtrymannia stalogo rozvytku v Karpatah. Naukovyj visnyk Uzhgorodskogo universytetu. Seria Biologia, 24, 5–10.

[7] Stojko, S. M. (2009). Dubovi lisy Ukrayinskyh Karpat: ekologichni osoblyvosti, vidtvorennia, ohorona. Lviv: Polli, 220.

[8] Chopyk, V. I., Fedoronchuk, M. M. (2015). Flora Ukrayinskyh Karpat. Ternopil: Terno-graf, 712.

[9] Panova, L. S., Protopopova, V. V., Morozuk, C. C. (2007). Vesniani roslyny Ukrainy. Ternopil: Navchalna knyga, 160.

[10] Hryhora, I. M., Yakubenko, B. Ye., Melnychuk, M. D. (2006). Heobotanika. Kyiv: Aristey, 448.

[11] Parnan, T. V. (2005). Migratsijni shliahy ta geneza arealu yalytsi biloji v golotseni za rezultatamy sporo-pylkovogo analizu. Ivano-Frankivsk, 210–213.

[12] Golubets, M. A. (2007). Retrospektyva i perspectyva lisovoi typologii. Lviv: Polli, 76.

[13] Onyshchenko, V. A. (2007). Zakonomirnosti poshyrennia vesnianyh efemeroidiv u shyrokolystianyh ta hvojnyh lisah Ukrainy. Urk. botan. zhurn., 64 (6), 806–824.

[14] Onyshchenko, V. A. (2009). Vydovyj sklad grabovo-dubovyh lisiv v rajoni kontaktu podilskoj ta prydniprovskoj asotsiatsij. Chernivtsi: Chernivetskij universytet, 68–72.

[15] Didukh, Ja. P. (2009). Chervona knyga Ukrainy. Roslynnyj svit. Kyiv: Globalkonsaltyng, 912.

[16] Gavrusevych, A. M., Brodovych, R. I., Rftsuliak, Yu. D. (2010). Dibrovy Ukrayinskyh Karpat I symizhnyh terytorij, jih stan ta osoblyvosti vidnovlennia. Ternopil: Pidruchnyky ta posibnyky, 160.

[17] Myklush, S. I. (2011). Rivnynni bukovi lisy Ukrainy. Lviv: ZUKTs, 260.

[18] Stojko, S. (2005). Characteristics of virgin forests of the Ukrainian Carpathians and their significance as ecological model for natural forest management. Natural Forests in the Temperate Zone of Europe – Values and utilization. Birmensdorf – Rakhiv, 423–430.

[19] Christensen, M., Hahn, K., Mountford, E. P., Ódor, P., Standovár, T., Rozenbergar, D. et. al (2005). Dead wood in European beech (Fagus sylvatica) forest reserves. Forest Ecology and Management, 210 (1–3), 267–282. doi: 10.1016/j.foreco.2005.02.032

[20] Commarmot, B., Brändli, U.-B., Hamor, F., Lavnyy, V. (Eds.) (2013). Inventory of the Largest Primeval Beech Forest in Europe. Rakhiv, 73. Available at: http://www.wsl.ch/dienstleistungen/publikationen/pdf/12494.pdf

IN SILICO MODELING OF THE REDOX METABOLISM IN HUMAN ERYTHROCYTES

Olga Dotsenko
Department of Biophysics
Donetsk National University
21 600-Richchya str., Vinnytsia, Ukraine, 21000
o.dotsenko@donnu.edu.ua

Abstract

There was elaborated the mathematical model of erythrocytes metabolism, including glycolysis (Embden-Meyerhof pathway), pentose phosphate pathway, metHb restoration pathway, H_2O_2 metabolism reaction. The final model includes 50 reactions and 60 metabolites. Within the model was studied the change of activity of some enzymes and concentrations of metabolites in stationary state, that take part in the processes of utilization of oxygen active forms and restoration of metgemoglobin, depending on amount of exogenous and endogenous H_2O_2. There was demonstrated the threshold character of changes of the many studied parameters, that testifies that the cells can be practically in physiological state at the change of external conditions for rather long time.

There was carried out an assessment of redox-state of erythrocytes at oxidizing load: was demonstrated the change of $E_{GSSG/2GSH}$ and from the concentration of endogenous H_2O_2. There was established that in the studied diapason of concentrations of endogenous H_2O_2 was observed the high slope of the change of $E_{GSSG/2GSH}$, that was not observed for and the other redox-pairs.

The results of modeling coincide with existing views on the functioning of enzymes of antioxidant protection in human erythrocytes and testify to the possibility of practical use of the model.

Keywords: erythrocytes, oxidizing stress, in silico modeling, redox potentials.

1. Introduction

Erythrocytes are often undergone the action of hydrogen peroxide (H_2O_2), that is referred to the oxygen active forms (OAF) and has a toxic effect on these cells. The base of peroxide toxicity is in its ability to disintegration with formation of highly reactive products, especially hydroxyl radical. The hydrogen peroxide in small concentrations (10^{-6}–10^{-7} M) at oxygen is able to initiate the oxidation of hemoglobin, and in result the number of oxidized heme-groups can significantly exceed the initial amount of peroxide. So far as the any oxyhemoglobin oxidation is connected with the production of active forms of oxygen and hydrogen peroxide, we must suggest that this process is an important link in methemoglobinemias development [1].

In this connection the redox-regulation of the cellular processes is the one of fundamental mechanisms of regulation of the cells functional activity. As the result of conjugated functioning of the systems of regeneration of oxygen active forms and antioxidizing protection and also membrane systems of transport of the different redox-molecules types the certain balance of the processes of accumulation and utilization of oxidizers and reoxidizers or redox-state is established in the cell. The support of this balance is vitally necessary for separate cells and organism as a whole [2].

It is possible to prognosticate the direction of redox-processes course and influence of the different physical-chemical factors on cell's redox-state with the help of the mathematical models, constructed using chemical kinetics laws.

The aim of the work is in elaboration of kinetic mathematical model for studying redox processes in erythrocytes on the base of the main carbonaceous metabolism made by Holzhütter [3].

2. Survey of the state of problem

Metabolic modeling is the promising approach for in silico prognostication of the ways of cell functioning on the base of interconnection and interaction of all cellular components [4].

There are two big classes of models, used for description and analysis of metabolic networks: stoichiometric and dynamic ones [5, 6]. Stoichiometric models are the detailed momentary picture of metabolic ways that are in stationary mode, established in given conditions. The dynamic models describe the changes of metabolites in time, using kinetic dependences for possibility to prognostication of changes in metabolism as the response on actions of external factors or genetic modifications [7].

For the better understanding of the work of cellular molecular networks at the system level (system biology) there were made many attempts of computed modeling of metabolic networks. Because of simplicity of structure, components and accessibility of kinetic information the metabolism of erythrocyte was the center of mathematical modeling for more than three decades and it is the main example of the use of mathematical modeling not only for understanding biochemical regulation but also as the base of constructing the other mathematical networks [6–11]. For example, the erythrocytes metabolism models were able to prognosticate the importance of glutathione de novo synthesis and its role in cells that have deficiency of glucose-6-phospate dehydrogenase (G6PDH) [7, 8], the results of enzymopathies of G6PDH and pyruvate kinase, to demonstrate the differences between patients with chronic and non-chronic anemia and deficiency of these two enzymes [7]. The erythrocytes metabolism models were used for analysis of physiological role of the two enzyme methemoglobin-restoring systems [9] and 3 band protein clustering processes at oxidizing stress [10] The one of the most known kinetic models of metabolism of human erythrocytes are Holzhütter [3] and Mulquiney & Kuchel models [11], that are freely accessible (http://www.jjj.bio.vu.nl/database).

3. Materials and Methods

The central carbonaceous metabolism is modeled using Holzhütter model [3], where 38 differential equations were constructed on the base of exact kinetic equations. This model was added with kinetic equations, describing the following processes:

1. Diffuse flows of exogenous O_2 and H_2O_2 are described by diffuse equations:

$$\nu_{O_2} = D_{O_2}\left(\left[O_2\_out\right]-\left[O_2\_in\right]\right), \quad (1)$$

where $\left[O_2\_out\right]=P_{O_2}\cdot k$, where P_{O_2} – partial pressure O_2 – 720 mm of mercury column, k – oxygen solubility in the blood plasma. Diffusion coefficient D_{O_2}=0,00684 h^{-1} [12].

$$\nu_{H_2O_2} = D_{H_2O_2}\left(\left[H_2O_2\_out\right]-\left[H_2O_2\_in\right]\right). \quad (2)$$

Diffusion coefficient $D_{H_2O_2}=15{,}12\ h^{-1}$ [13]. Extracellular concentration of hydrogen peroxide $\left[H_2O_2\_out\right]=10^{-4}$ mM/l, $\left[H_2O_2\_in\right]=10^{-9}$ mM/l.

2. Oxygenation processes were described according to [12]:

$$\nu = K_{дис}\cdot k_2\left[O_2\_in\right]^n\left[Hb\right]-k_2\left[HbO_2\right], \quad (3)$$

where: $K_{дис}$ – constant of oxyhemoglobin dissociation – 2030, k_2 – constant of the speed of oxyhemoglobin dissociation reaction – 1584 1/h, n-cooperativeness degree – 3.

3. Generation of intracellular superoxydanion-radical and hydrogen peroxide:

3. 1. Process of hemoglobin autoxidation:

$$\nu_{O_2^-\cdot} = k\cdot\left[HbO_2\right], \quad (4)$$

k – constant of the speed of oxyhemoglobin autoxidation reaction – 1×10^{-5} h^{-1} [14].

3. 2. Processes of endogenous hydrogen peroxide regeneration:

3. 2. 1. Hemoglobin oxidation

$$\nu\cdot = k\cdot[Hb]\cdot[O_2^-\cdot], \quad (5)$$

k – constant of the reaction speed, 14400 $mM^{-1}\times h^{-1}$ [14].

3. 2. 2. Glutathione autoxidation:

$$\nu\cdot = k\cdot[GSH]^2\cdot[O_2\_in], \quad (6)$$

k – constant of reaction speed – 0,36 $mM^{-2}h^{-1}$ [15].

3. 2. 3. Dismutation reaction $O_2^-\cdot$ with participation of superoxide dismutase:

$$\nu\cdot = k\cdot[O_2^-\cdot]^2, \quad (7)$$

k – constant of the speed of the second-order reaction – $300\,mM^{-1}h^{-1}$ [15].

4. Inactivation of endogenous hydrogen peroxide in reactions catalyzed by catalase and glutathione peroxidase:

4. 1. Reaction, catalyzed by catalase:

$$\nu\cdot = k\cdot[H_2O_2]^2, \quad (8)$$

k – constant of the speed of second-order reaction – $7{,}5\times10^6$ $mM^{-1}\times h^{-1}$ [16].

4. 2. Reaction, catalyzed by glutathione peroxidase:

$$\nu\cdot = \frac{[GP_x]}{\frac{k_1}{[H_2O_2\_in]}+\frac{k_2}{[GSH]}}. \quad (9)$$

The conclusion of equation was described in [17], $[GP_x]$ – glutathione peroxidase concentration $9{,}7\times10^{-4}$ mM. $k_1=1{,}32\times10^{-8}$, $k_2=6{,}97\times10^{-6}$.

5. Processes of methemoglobin restoration were described by equations offered in [17], metabolites concentrations and parameters values were taken from this work.

Scheme of the network used in the work is demonstrated on the **Fig. 1.**

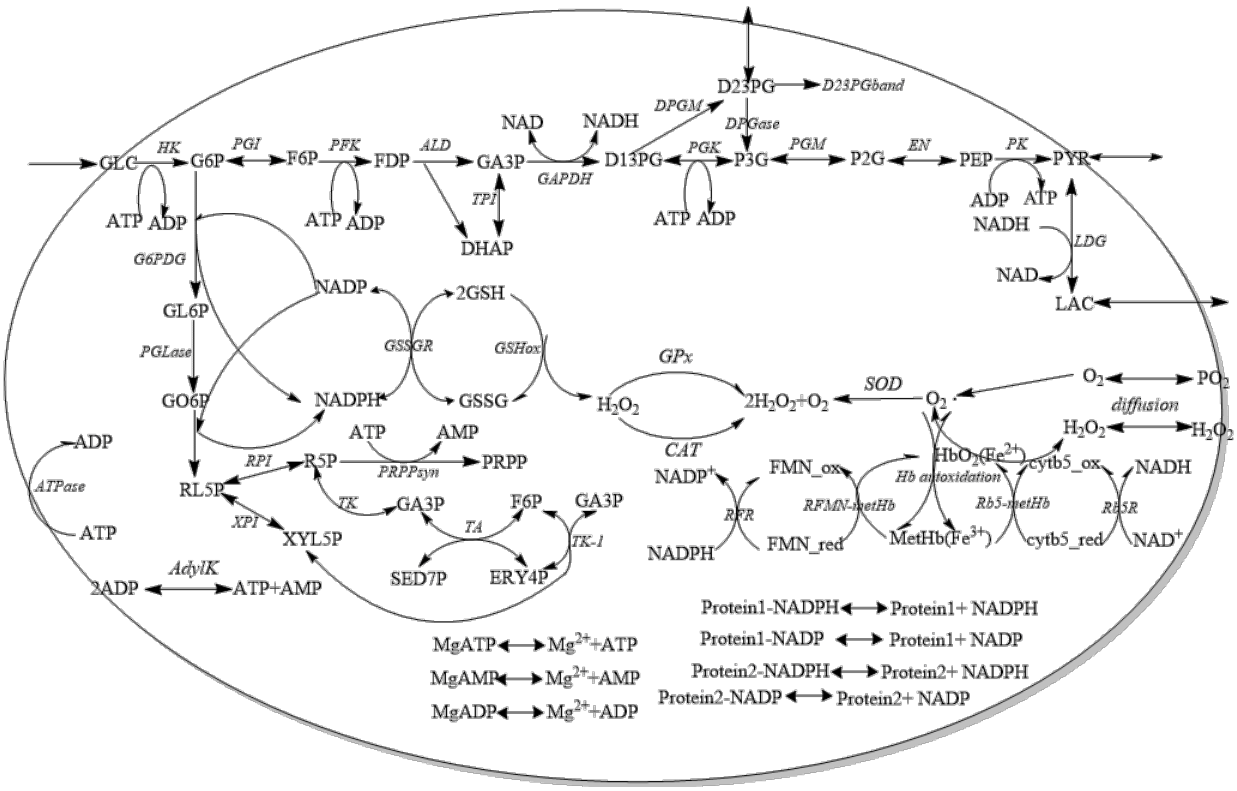

Fig. 1. Schematic representation of the pathways included in the model: **Metabolite:** GLC, glucose; G6P, glucose 6-phosphate; F6P, fructose 6-phosphate; FDP, fructose 1,6-diphosphate; DHAP, dihydroxyacetone phosphate; GA3P, glyceraldehyde 3-phosphate; D13PG, 1,3-diphosphoglycerate; D23PG, 2,3-diphosphoglycerate; D23PGband, band-form 2,3-diphosphoglycerate; P2G, 2-phosphoglycerate; P3G, 3-phosphoglycerate; PEP, phosphenolpyruvate; PYR, pyruvate; LAC, lactate; GL6P, gluconolactone 6-phosphate; GO6P, gluconate 6-phosphate; RU5P, ribulose 5-phosphate; R5P, ribose 5-phosphate; X5P, xylulose 5-phosphate; S7P, sedoheptulose 7-phosphate; E4P, erythrose 4-phosphate; GSH, reduced glutathione; GSSG, oxidized glutathione; H_2O_2, hydrogen peroxide, HbO_2, oxyhemoglobin, MetHb , methemoglobin; O_2, oxygen; $O_2^-\cdot$, superoxide anion radical; cytb5_ox, oxidized cytochrome b5; cytb5_red, reduced form cytochrome b5. **Enzymes:** HK, hexokinase (EC 2.7.1.1), PGI, glucose-6-phosphate isomerase (EC 5.3.1.9); PFK, phosphofructokinase (EC 2.7.1.11); ALD, aldolase (EC 4.1.2.13); TPI, triosephosphate isomerase (EC 5.3.1.1); GAPDH, glyceraldehyde-3-phosphate dehydrogenase (EC 1.2.1.12); PGK, phosphoglycerate kinase (EC 2.7.2.3); DPGase, diphosphoglycerate phosphatase (EC 3.1.3.13); PGM, phosphoglycerate mutase (EC 5.4.2.1); EN, enolase (EC 4.2.1.11); PK, pyruvate kinase (EC 2.7.1.40); LDG, lactate dehydrogenase (EC 1.1.1.27); G6PDH, glucose-6-phosphate dehydrogenase (EC 1.1. 1.49) GAPDH, glyceraldehyde-3-phosphate dehydrogenase (EC 1.2.1.12); GL6PDH, phosphogluconate dehydrogenase (EC 1.1.1.44), RPI, ribose-5-phosphate isomerase (EC 5.3.1.6); XPI, ribulose phosphate epimerase (EC 5.1.3.1); TA, transaldolase (EC 2.2.1.2); TK, transketolase (EC 2.2.1.1); PRPPsyn, phosphoribosylpyrophosphate synthetase (EC 2.7.6.1); cytb5R, (NADH-dependent) cytochrome b5 reductase (EC 1.6.2.2); FR, (NADPH-dependent) flavin reductase (EC 1.5.1.30); GPx, glutathione peroxidase (EC 1.11.1.9); SOD, Superoxide dismutase (EC 1.15.1.1), CAT- catalase (1.11.1.6); GSSGR, glutathione-disulfide reductase (EC 1.8.1.7); GSHox –glutathione autoxidation reaction

4. Experimental procedures

Model was created in COPASI program. Instruments of this program support the modeling procedure, guaranteeing the flexible system of changes of parameters values [18]. The final model includes 50 reactions and 60 metabolites and consists of glycolysis reactions, 2,3-biphosphoglycerate shunt, pentose phosphate pathway, MetHb restoration pathways and the few obligatory processes of interaction of hemoglobin with metabolites (for example, ATP 2,3-biphosphoglycerate) and metabolism reactions of the hydrogen peroxide. The oxidizing load on erythrocyte was modeled changing the amount of exogenous H_2O_2.

Mathematical methods used in the work:

1. Calculation of stationary concentrations and reaction flows for verification of adequacy of elaborated model.

2. The scanning of parameters. This procedure was used for the study of sensitivity of reaction flows and metabolites of model to the value of extracellular H_2O_2 that reflects intensity of oxidizing load on the cell.

5. Results and Discussion

The calculations demonstrated that the change of H_2O_2 content in interval of 10^{-6}–10^{2} mM results in the change of endogenous H_2O_2 content 10^{-8}–10^{-2} mM. The change of reaction flows and metabolites concentrations was analyzed depending on endogenous H_2O_2.

The data of modeling demonstrated that an increase of oxidizing load on the cell results in increase of flow through the Embden-Meyerhof pathway but if the flow through hexokinase increases in 2 times (**Fig. 2,** ***dependence 1***), the increase of the flow through glyceraldehyde phosphate dehydrogenase is 17 % of the initial value (**Fig. 2**, ***dependence 4***), that is connected with the reverse of flow at the level of glucosephosphatimerase and reorientation of the glycolytic flow to the pentose phosphate pathway (**Fig. 2**, ***dependence 2***). At the increase of oxidizing load there is registered also the displacement of catalyzed LDG to the pyruvate side (**Fig. 2**, ***dependence 3***). It is well known that in conditions of surplus oxidation the risen demand for NADH is connected with the prevalence of the reverse lactadehydrogenase (LDG) reaction. The pyruvate accumulation in plasma as the result of the pyruvate/lactate shuttle in erythrocytes in the conditions of surplus oxidation and MetHb increase is experimentally proved [9].

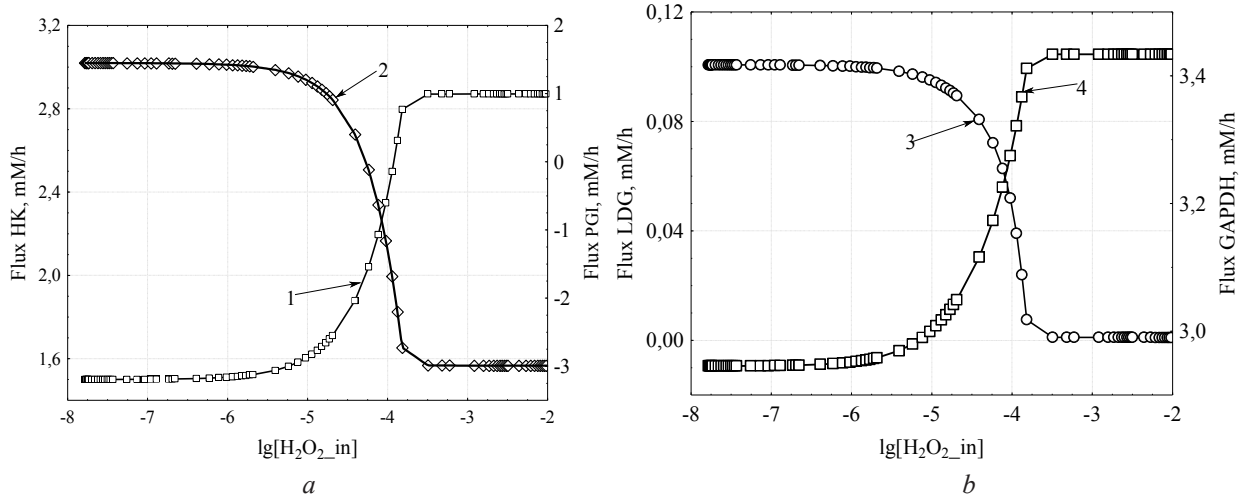

a *b*

Fig. 2. The change of enzyme activity in stationary state in conditions of oxidizing load: *a* – HK (1), PGI (2); *b* – LDG (3), GAPDH (4)

In conditions of the oxidizing load the flow through G6PDG essentially increases, that is connected with the necessity to support the certain NADPH level as the restoring equivalent. According to the modeling data, the flow through G6PDG increases in 6 times at extracellular H_2O_2 content exceeding 10^{-4} mM (**Fig. 3,** ***a***, ***dependence 2***). It is well known, that G6PDG has the surplus activity [8] that allows support the high NADPH and GSH level at the surplus oxidizing load.

According to the received data, the increase of intracellular H_2O_2 content to 10^{-4} mM is the critical one and results in abrupt decrease of both NADPH and GSH content in cell despite the high activity of G6PDG and glutathione reductase (GR) (**Fig. 3, *a***, ***dependencies 2, 3***). The increase of NADP concentration (**Fig. 3, *b***, ***dependence 2***) can be explained by the intensive use of NADPH in the other reactions, especially for methemoglobin restoration and glutathione oxidized by glutathione reductase, which concentration also increases at oxidizing load (**Fig. 4, *a***).

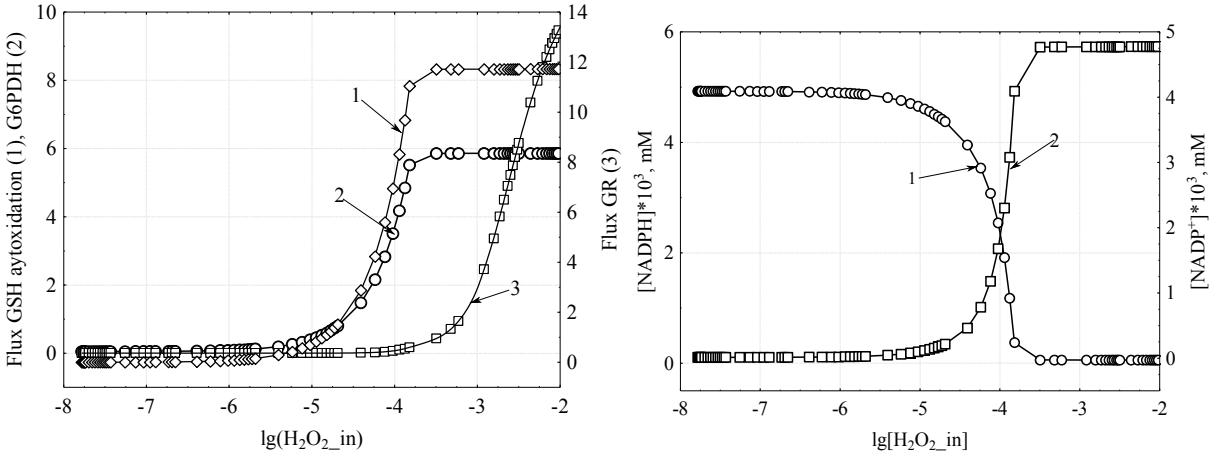

Fig. 3. The change of flows and stationary concentrations of metabolites in conditions of oxidizing load: *a* – autoxidation GSH (1), G6PDH (2); *b* – [NADPH] (2) and [NADP+] (1)

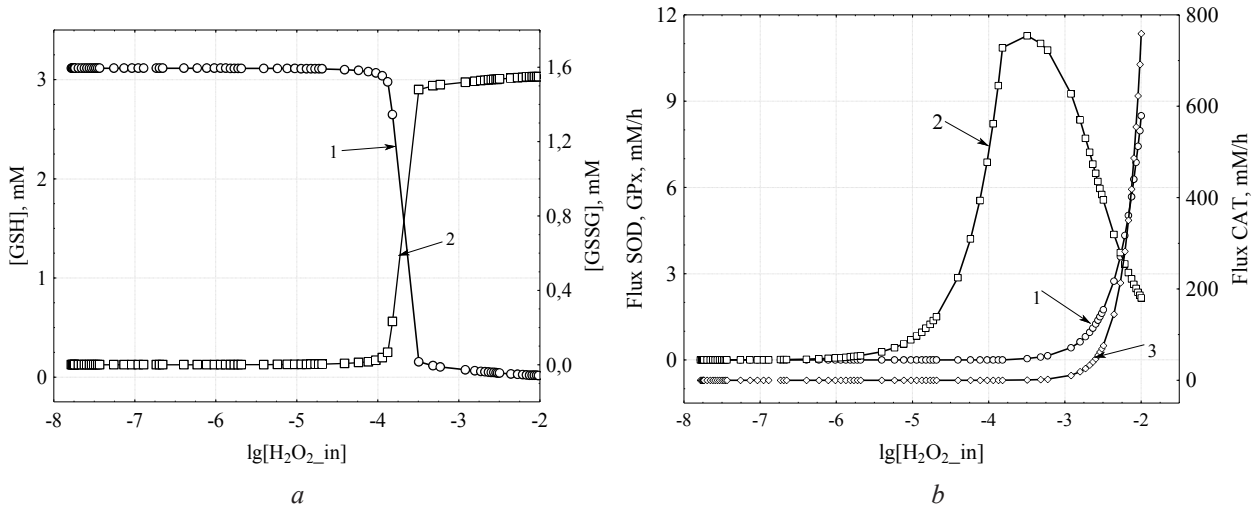

Fig. 4. The change of flows and stationary concentrations of metabolites in conditions of oxidizing load: *a* – [GSH] (1) and [GSSG] (2); *b* – CAT (1), GPx (2), SOD (3)

The protection of erythrocyte from oxidizing load probably plays the significant role in the life of these cells. In this connection the system of restoring equivalents production has the practically threshold behavior at the increase of oxidizers content. It means that to the certain values of oxidizing load the system can be in the practically physiological state for the rather long time by the degree of GSH and NADPH restoration.

In fact the main mission of the source of NADPH restoring equivalents in erythrocytes is the transformation of the oxidized glutathione form (GSSG) into its restored form (GSH) in reaction, catalyzed by the glutathione reductase. GSH is necessary to avoid the irreversible oxidation of intracellular proteins, including membrane proteins and enzymes whereas GSSG accumulation causes the protein dysfunction as the result of creation of disulfide connections between SH-cyste-

ine groups and methionine residuals [19]. That is why the high activities of G6PDH and glutathione reductase in human erythrocytes are evolutionary determined to avoid the intense NADPH emaciation and GSSG accumulation at oxidizing load [8].

On the **Fig. 4, *b*** is demonstrated the change of enzymes, inactivating the surplus amount of H_2O_2 and O_2^-. The modeling data are well agreed with the literature data on the fact, that the first glutathione peroxidase works more effectively at the low substrate concentrations, whereas in cells protection from oxidizing stress, caused by the high hydrogen peroxide concentrations, the node role belongs to catalase [17].

On the **Fig. 5.** is demonstrated the change of redox-potentials of GSSG/2GSH, NAD^+/NADH and $NADP^+$/NADPH pairs at the increase of oxidizing load.

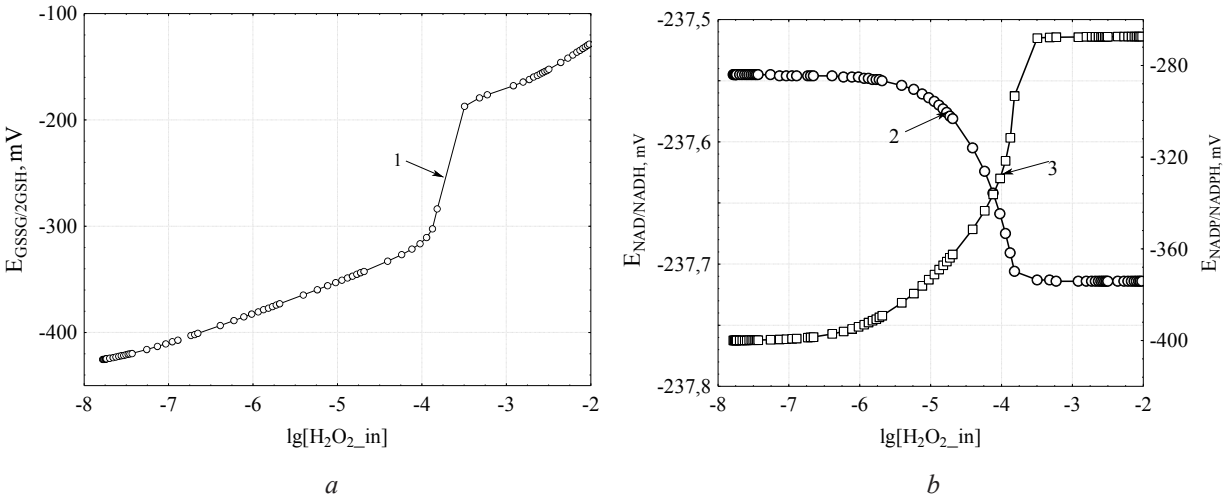

Fig. 5. The change of redox-potentials at oxidizing load:
a – redox-potential GSSG/2GSH; *b* – NAD+/NADH (1) and NADP+/NADPH (2)

Redox-potentials for GSSG/2GSH pair are more sensitive to the change of endogenous H_2O_2 content, especially in the range of its high concentrations (10^{-4}–10^{-2} mM). For this range of H_2O_2 concentrations is typical the high slope of $E_{GSSG/2GSH}$ change, that is not observed for $E_{NADP^+/NADPH}$. As to $E_{NAD^+/NADH}$, the essential changes of this parameter were not detected at work.

Kinetics of GSSG/2GSH pair interaction, conjugated with others redox-active systems, for example, with $NADP^+$/NADPH, is not sufficient for attaining balance in ordinary biological conditions. According to the calculations, $E_{GSSG/2GSH}$ changes in diapason −400 – −100 мV and $E_{NADP^+/NADPH}$ is in the range −400 – −270 mV. It is possibly connected with the fact, that GR has the relatively high Km for GSSG, so its activity is limited by the speed of GSSG restoration in the normal cells. In this case the stationary speed of GSH oxidation is sufficient for support of oxidizing-restoring balance of GSSG/2GSH pair that essentially changes comparing with $NADP^+$/NADPH [20]. The existent literary data demonstrate that the oxidizing-restoring state of GSSG/2GSH pair is surprisingly similar in the different cellular types and can play the central role in the cellular metabolism regulation.

6. Conclusions

In the cell function mechanisms, directed on the support of certain, typical for this cell, balance of processes of accumulation and utilization of electrons donors and acceptors. As the result of the work of these mechanisms the redox-homeostasis of cells is supported. The system of production of restoring equivalents has practically threshold behavior at the increase of oxidizers content. The cellular redox-homeostasis is supported by the work of these mechanisms.

References

[1] Rifkind, J. M., Nagababu, E. (2013). Hemoglobin Redox Reactions and Red Blood Cell Aging. Antioxidants & Redox Signaling, 18 (17), 2274–2283. doi: 10.1089/ars.2012.4867

[2] Martinovich, G. G., Martinovich, I. V., Cherenkevich, S. N., Sauer, H. (2010). Redox Buffer Capacity of the Cell: Theoretical and Experimental Approach. Cell Biochemistry and Biophysics, 58 (2), 75–83. doi: 10.1007/s12013-010-9090-3

[3] Holzhütter, H.-G. (2004). The principle of flux minimization and its application to estimate stationary fluxes in metabolic networks. European Journal of Biochemistry, 271 (14), 2905–2922. doi: 10.1111/j.1432-1033.2004.04213.x

[4] Bulik, S., Grimbs, S., Huthmacher, C., Selbig, J., Holzhütter, H. G. (2008). Kinetic hybrid models composed of mechanistic and simplified enzymatic rate laws - a promising method for speeding up the kinetic modelling of complex metabolic networks. FEBS Journal, 276 (2), 410–424. doi: 10.1111/j.1742-4658.2008.06784.x

[5] Schuster, S., Klamt, S., Weckwerth, W., Moldenhauer, F., Pfeiffer, T. (2002). Use of network analysis of metabolic systems in bioengineering. Bioprocess and Biosystems Engineering, 24 (6), 363–372. doi: 10.1007/s004490100253

[6] Yachie-Kinoshita, A., Nishino, T., Shimo, H., Suematsu, M., Tomita, M. (2010). A Metabolic Model of Human Erythrocytes: Practical Application of the E-Cell Simulation Environment. Journal of Biomedicine and Biotechnology, 2010, 1–14. doi: 10.1155/2010/642420

[7] Shimo, H., Nishino, T., Tomita, M. (2011). Predicting the Kinetic Properties Associated with Redox Imbalance after Oxidative Crisis in G6PD-Deficient Erythrocytes: A Simulation Study. Advances in Hematology, 2011, 1–10. doi: 10.1155/2011/398945

[8] Salvador, A., Savageau, M. A. (2003). Quantitative evolutionary design of glucose 6-phosphate dehydrogenase expression in human erythrocytes. Proceedings of the National Academy of Sciences, 100 (24), 14463–14468. doi: 10.1073/pnas.2335687100

[9] Kinoshita, A., Nakayama, Y., Kitayama, T., Tomita, M. (2007). Simulation study of methemoglobin reduction in erythrocytes. FEBS Journal, 274 (6), 1449–1458. doi: 10.1111/j.1742-4658.2007.05685.x

[10] Shimo, H., Arjunan, S. N. V., Machiyama, H., Nishino, T., Suematsu, M., Fujita, H. et. al (2015). Particle Simulation of Oxidation Induced Band 3 Clustering in Human Erythrocytes. PLOS Computational Biology, 11 (6), e1004210. doi: 10.1371/journal.pcbi.1004210

[11] Mulquiney, P. J., Kuchel, P. W. (1999). Model of 2,3-bisphosphoglycerate metabolism in the human erythrocyte based on detailed enzyme kinetic equations1: equations and parameter refinement. Biochemical Journal, 342 (3), 581–596. doi: 10.1042/bj3420581

[12] Dash, R. K., Korman, B., Bassingthwaighte, J. B. (2015). Simple accurate mathematical models of blood HbO2 and HbCO2 dissociation curves at varied physiological conditions: evaluation and comparison with other models. European Journal of Applied Physiology, 116 (1), 97–113. doi: 10.1007/s00421-015-3228-3

[13] Low, F. M., Hampton, M. B., Peskin, A. V., Winterbourn, C. C. (2007). Peroxiredoxin 2 functions as a noncatalytic scavenger of low-level hydrogen peroxide in the erythrocyte. Blood, 109 (6), 2611–2617. doi: 10.1182/blood-2006-09-048728

[14] Johnson, R., Goyettejr, G., Ravindranath, Y., Ho, Y. (2005). Hemoglobin autoxidation and regulation of endogenous H2O2 levels in erythrocytes. Free Radical Biology and Medicine, 39 (11), 1407–1417. doi: 10.1016/j.freeradbiomed.2005.07.002

[15] Scarpa, M., Momo, F., Viglino, P., Vianello, F., Rigo, A. (1996). Activated oxygen species in the oxidation of glutathione A kinetic study. Biophysical Chemistry, 60 (1-2), 53–61. doi: 10.1016/0301-4622(96)00002-6

[16] Tao, Z., Raffel, R. A., Souid, A.-K., Goodisman, J. (2009). Kinetic Studies on Enzyme-Catalyzed Reactions: Oxidation of Glucose, Decomposition of Hydrogen Peroxide and Their Combination. Biophysical Journal, 96 (7), 2977–2988. doi: 10.1016/j.bpj.2008.11.071

[17] Ng, C. F., Schafer, F. Q., Buettner, G. R., Rodgers, V. G. J. (2007). The rate of cellular hydrogen peroxide removal shows dependency on GSH: Mathematical insight into in vivo H_2O_2 and GPx concentrations. Free Radical Research, 41 (11), 1201–1211. doi: 10.1080/10715760701625075

[18] Mendes, P., Hoops, S., Sahle, S., Gauges, R., Dada, J., Kummer, U. (2009). Computational Modeling of Biochemical Networks Using COPASI. Systems Biology, 17–59. doi: 10.1007/978-1-59745-525-1_2

[19] Biswas, S., Chida, A. S., Rahman, I. (2006). Redox modifications of protein–thiols: Emerging roles in cell signaling. Biochemical Pharmacology, 71 (5), 551–564. doi: 10.1016/j.bcp.2005.10.044

[20] Jones, D. P. (2002). [11] Redox potential of GSH/GSSG couple: Assay and biological significance. Methods in Enzymology, 93–112. doi: 10.1016/s0076-6879(02)48630-2